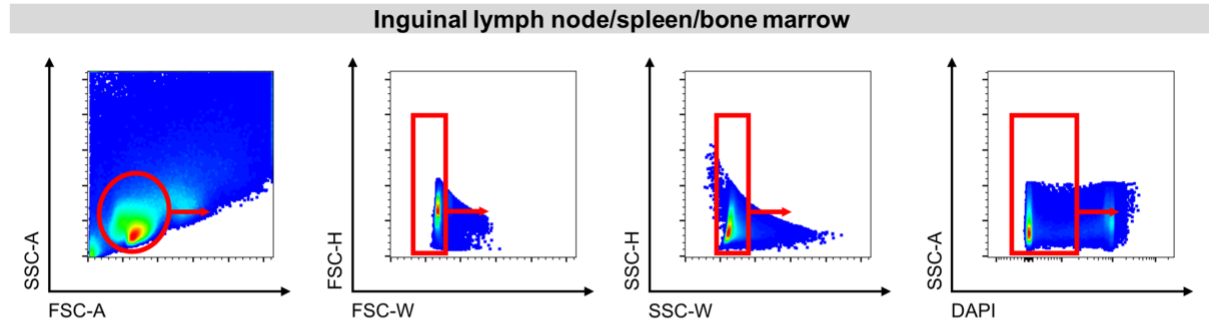
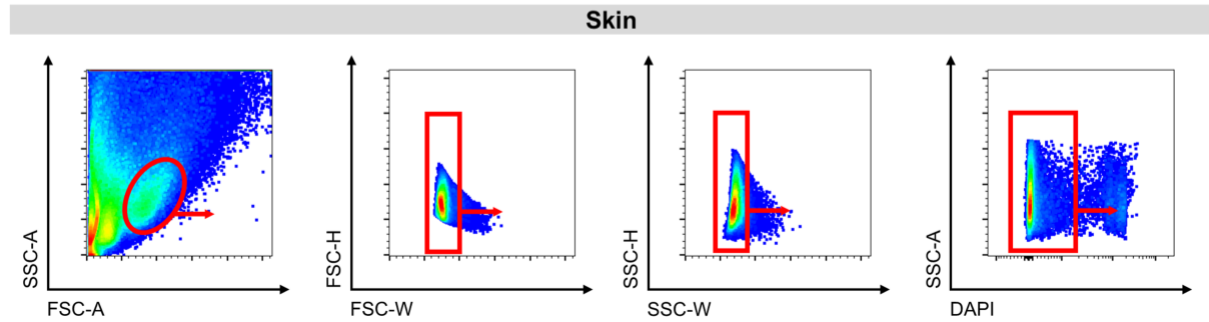


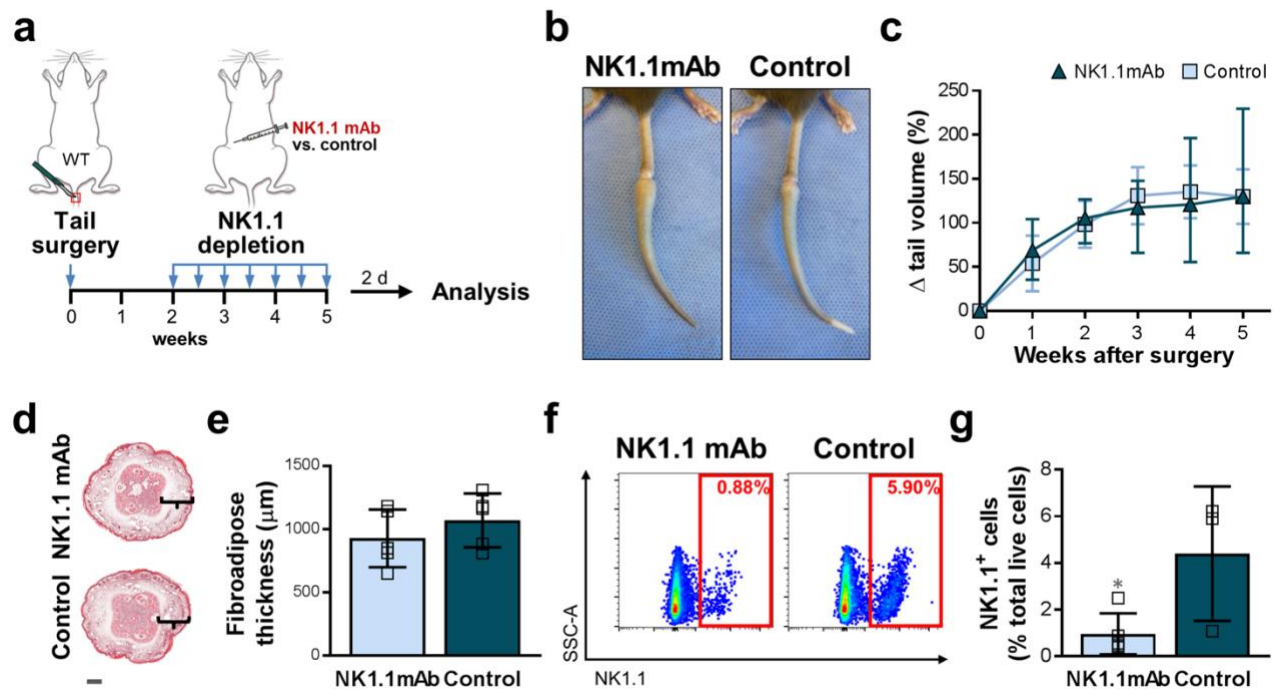
## **Supplementary Figures**

**CD4<sup>+</sup> T cells are activated in regional lymph nodes and home to skin to initiate lymphedema**

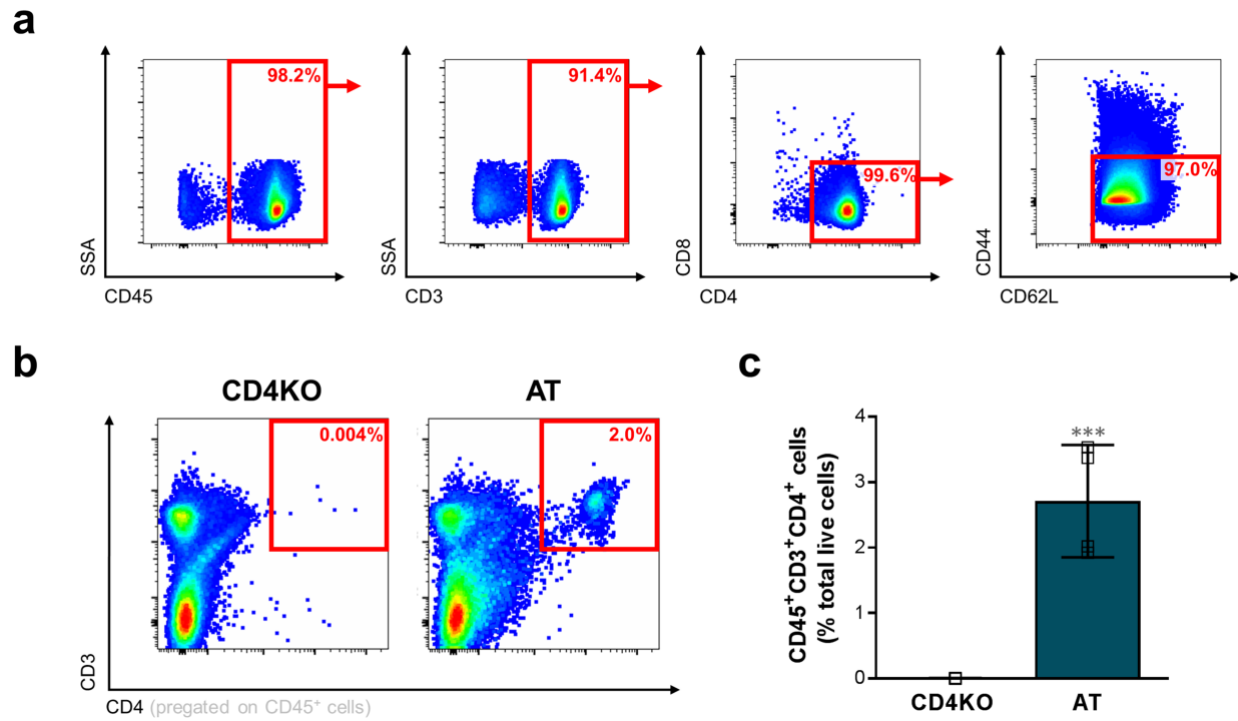
García Nores et al.

**a****b**

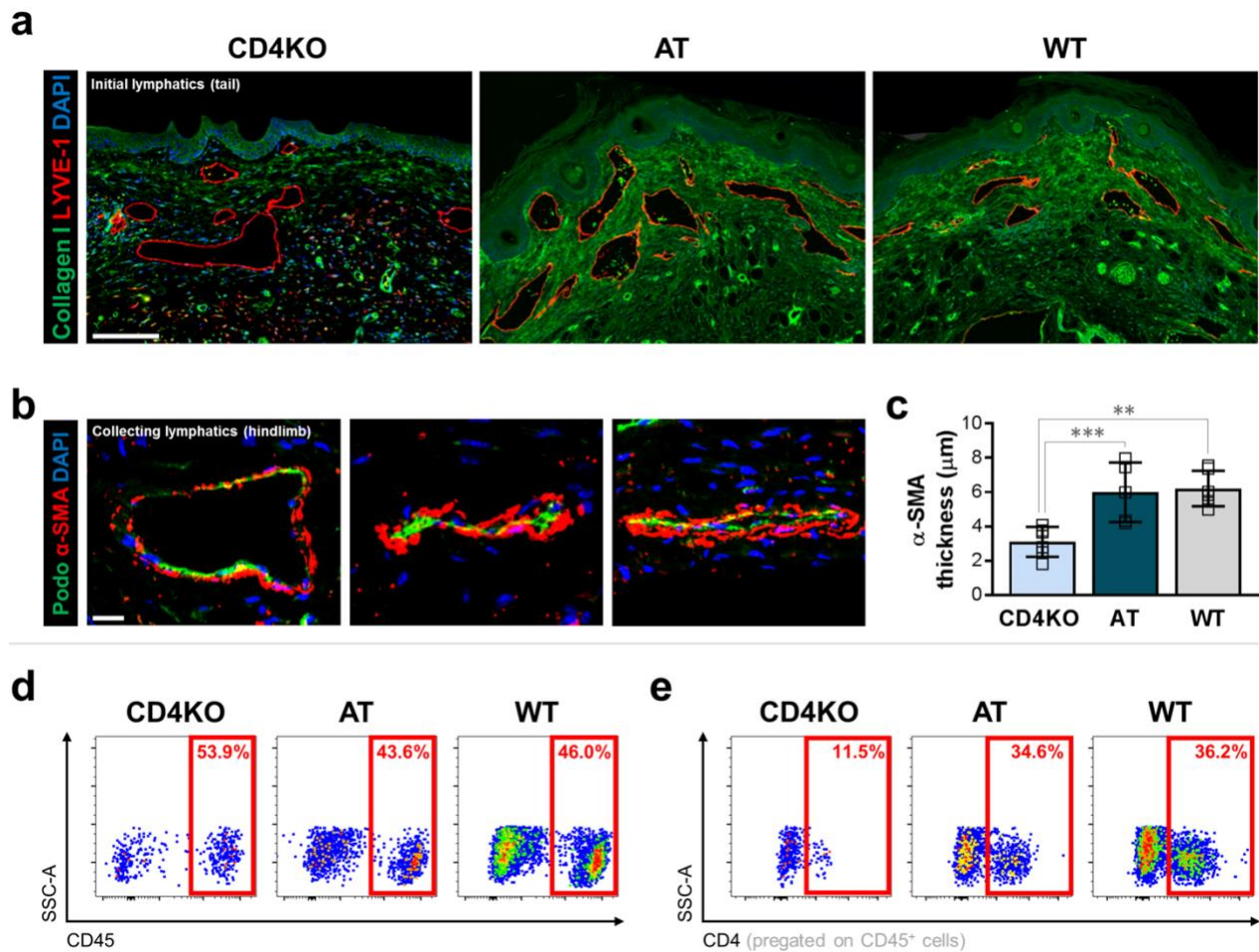
**Supplementary Fig. 1. Gating strategy for flow cytometry.** **a, b** CD4<sup>+</sup> T cells and subsets were identified in single-cell suspensions obtained from ipsilateral inguinal lymph nodes, spleen, bone marrow (**a**), and skin from the tail or hindlimb distal to the surgical site (**b**) following tail skin and lymphatic excision or popliteal lymph node dissection, respectively, using a standard gating strategy. This gating strategy was utilized for Fig. 2b, 2d, 2f, 3b-c, 3e, 8d-e; Supplementary Fig. 1f, 2a-b, 3d-e, and 7.



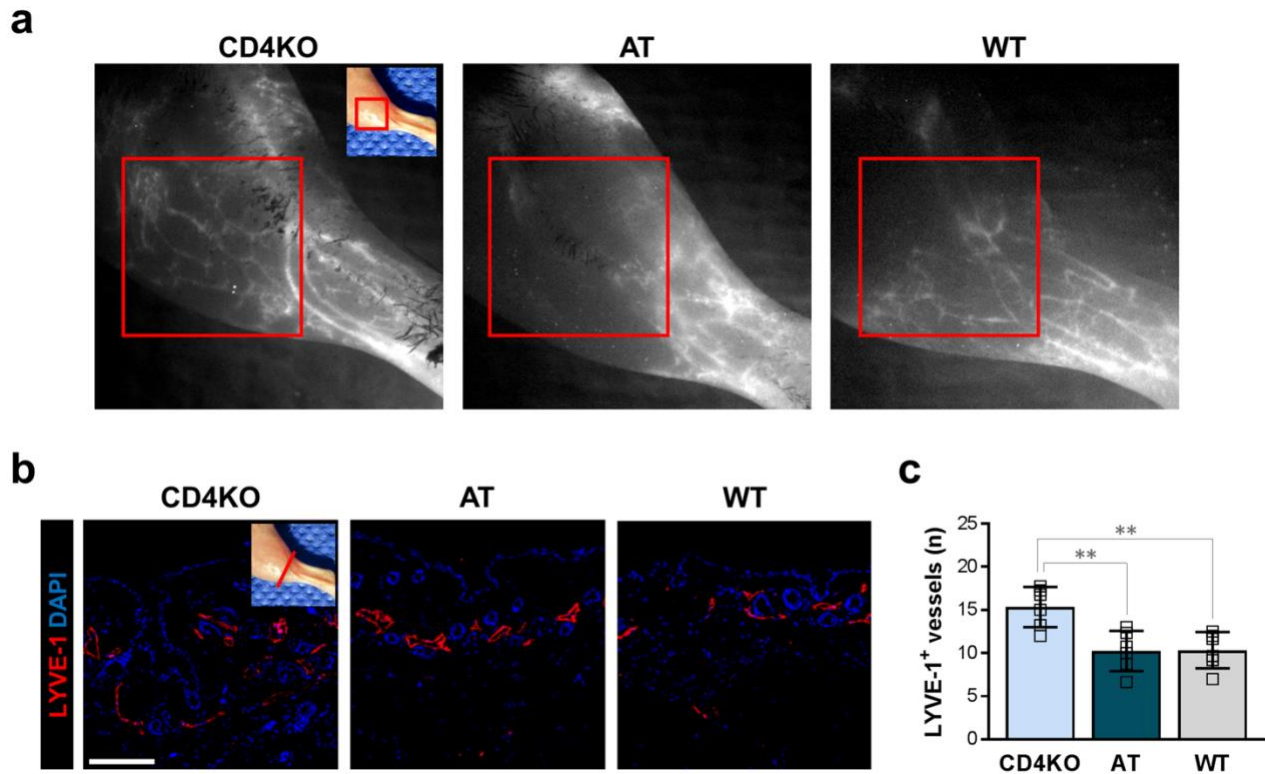
**Supplementary Fig. 2. NK1.1 depletion does not reverse lymphedema.** **a** Schematic diagram of treatment with neutralizing antibodies to NK1.1 or isotype control following tail skin and lymphatic excision. Mice sacrificed 37 days after surgery. **b** Representative photographs of tails five weeks after surgery. **c** Quantification of tail volume change (n=5/group). **d** Representative H&E staining of tail cross-sections with brackets indicating fibroadipose tissue; scale bar, 1000  $\mu\text{m}$ . **e** Quantification of fibroadipose thickness (n=5/group; 5 hpf/mouse). **f** Representative FACS plots (*left*) and quantification (*right*) of single, live NK1.1<sup>+</sup> cells in tail skin (n=3 for control group, n=6 for NK1.1 mAb group). Data representative of a minimum of 2 independent experiments with similar results; statistical analyses of one experiment shown. Mean  $\pm$  s.d.; \* $P$ <0.05 by two-way ANOVA or unpaired student's t test. H&E, hematoxylin and eosin; hpf, high-powered field.



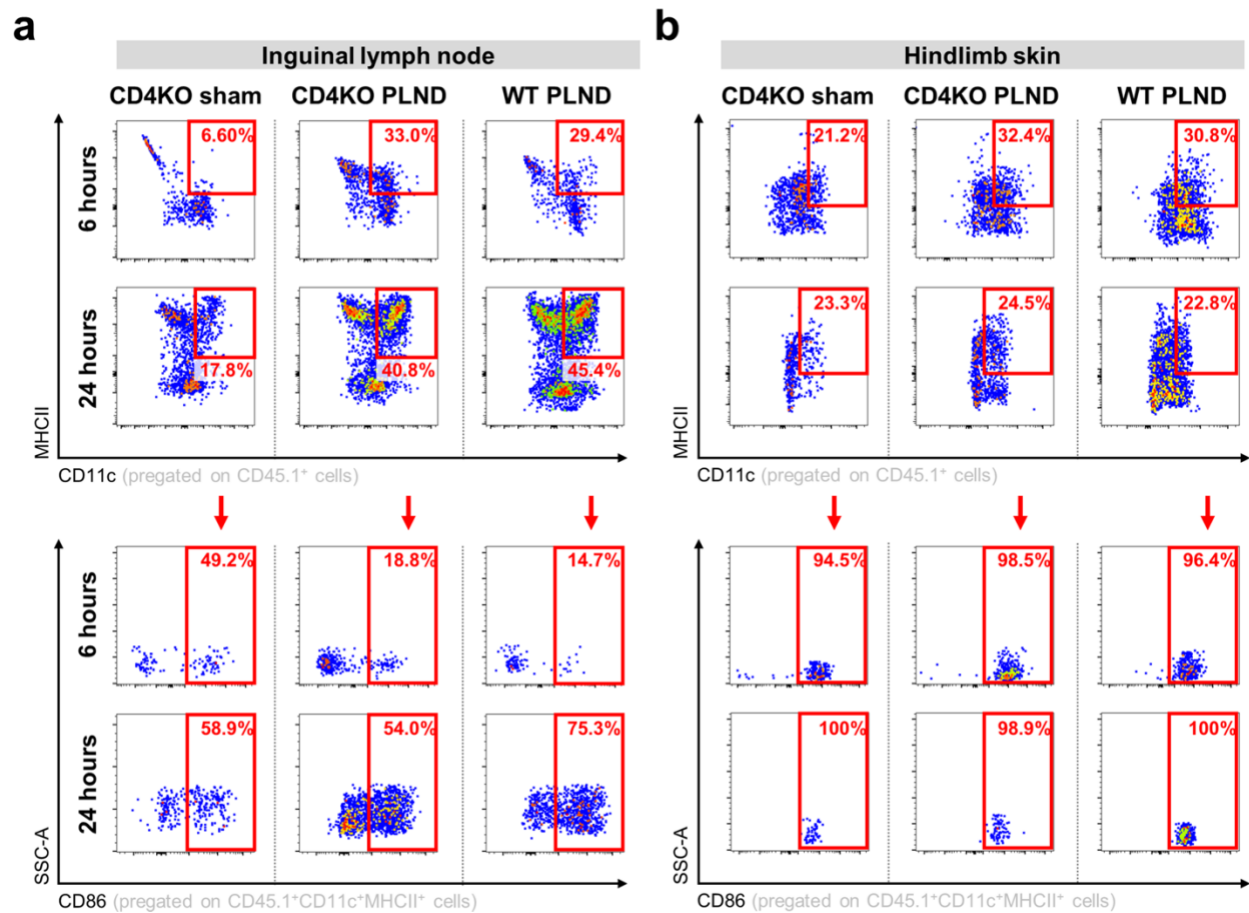
**Supplementary Fig. 3. Naïve CD4<sup>+</sup> T cells were successfully isolated and transferred to CD4KO mice. a** Representative FACS plots depicting the gating strategy utilized to identify single, live CD45<sup>+</sup>CD3<sup>+</sup>CD4<sup>+</sup>CD44<sup>+</sup>CD62L<sup>+</sup> cells in single-cell suspensions of cells isolated from WT mouse spleens by magnetic bead negative selection. **b, c** Representative FACS plots (**b**) and quantification (**b**) of single, live CD45<sup>+</sup>CD3<sup>+</sup>CD4<sup>+</sup> cells in the spleens of CD4KO and AT mice (n=4 for AT group, n=5 for CD4KO group; mean ± s.d.; \*\*\**P*=0.0002 by unpaired student's t test). Data representative of a minimum of 2 independent experiments with similar results; statistical analyses of one experiment shown. AT, CD4KO mice that underwent adoptive transfer with naïve CD4<sup>+</sup> T cells.



**Supplementary Fig. 4. Adoptive transfer of CD4<sup>+</sup> T cells to CD4KO mice results in increased fibrosis and local inflammation in area of lymphatic injury.** Mice sacrificed 6 weeks after tail skin and lymphatic excision or 4 weeks after PLND. **a** Representative immunofluorescent images of tail cross-sections co-localizing LYVE-1<sup>+</sup> initial lymphatic vessels with type I collagen; scale bar, 200  $\mu\text{m}$ . **b** Representative immunofluorescent images of hindlimb collecting lymphatic vessels co-localizing podoplanin and  $\alpha$ -SMA; scale bar, 100  $\mu\text{m}$ . **c** Quantification of  $\alpha$ -SMA thickness ( $n=6/\text{group}$ ; 4 hpf/mouse; mean  $\pm$  s.d.; \*\* $P<0.01$  and \*\*\* $P<0.001$  by one-way ANOVA with Tukey's multiple comparisons test). **d**, **e** Representative FACS plots of single, live CD45<sup>+</sup> (**d**) and CD45<sup>+</sup>CD4<sup>+</sup> cells (**e**) in tail skin. Data representative of a minimum of 2 independent experiments with similar results; statistical analyses of one experiment shown.  $\alpha$ -SMA, alpha smooth muscle actin; AT, CD4KO mice that underwent adoptive transfer with naïve CD4<sup>+</sup> T cells; hpf, high-powered field; PLND, popliteal lymph node dissection.

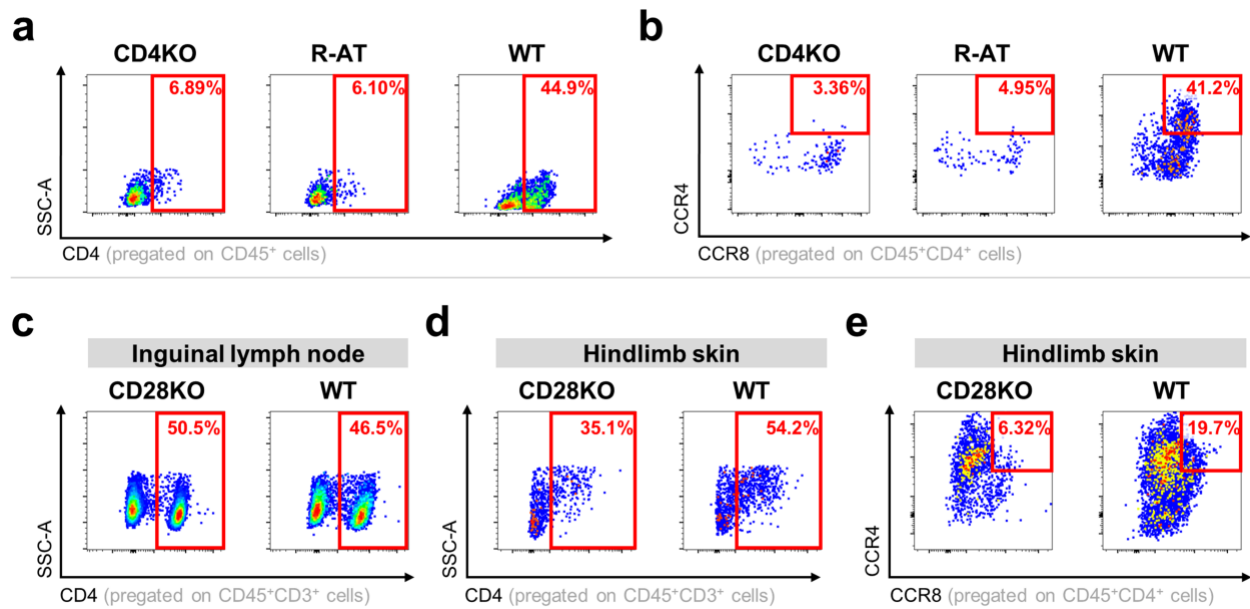


**Supplementary Fig. 5. Adoptive transfer of CD4<sup>+</sup> T cells to CD4KO mice results in decreased collateral vessel formation.** Mice analyzed 4 weeks after PLND. **a** Representative lymphangiography images after ICG injection with red squares indicating the presence of collateral vessel formation in CD4KO mice and the absence in AT and WT mice. **b** Representative immunofluorescent images localizing LYVE-1<sup>+</sup> initial lymphatic vessels with inset for anatomic correlation; scale bar, 200  $\mu$ m. **c** Quantification of LYVE-1<sup>+</sup> vessels per 0.25 mm<sup>2</sup> (n=6/group; 4 hpf/mouse; mean  $\pm$  s.d.; \*\* $P$ <0.01 by one-way ANOVA with Tukey's multiple comparisons test). Data representative of a minimum of 2 independent experiments with similar results; statistical analyses of one experiment shown. AT, CD4KO mice that underwent adoptive transfer with naïve CD4<sup>+</sup> T cells; hpf; high-powered field; ICG, indocyanine green.



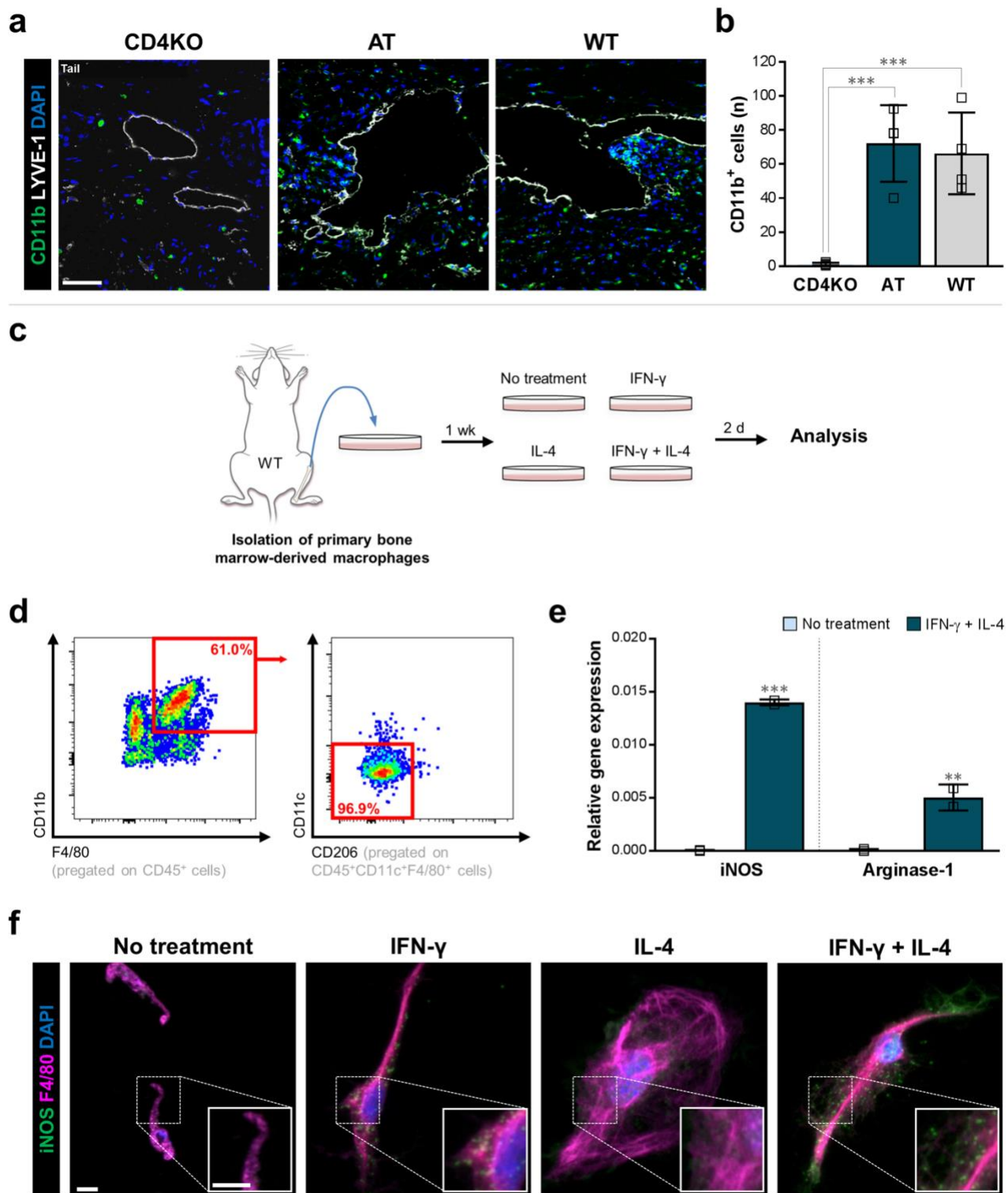
**Supplementary Fig. 6. Adoptively transferred DCs are initially activated in the skin after lymphatic injury.** **a, b** Representative FACS plots of single, live CD45.1<sup>+</sup>CD11c<sup>+</sup>MHCII<sup>+</sup> DCs (*upper*) further characterized into activated CD45.1<sup>+</sup>CD11c<sup>+</sup>MHCII<sup>+</sup>CD86<sup>+</sup> DCs (*lower*) in the ipsilateral inguinal lymph nodes (**a**) and hindlimb skin (**b**) of mice depicted in Fig. 5a. DCs, dendritic cells; PLND, popliteal lymph node dissection.





**Supplementary Fig. 7. T cell activation is required for the development of lymphedema.** **a, b** Representative FACS plots of single, live CD45<sup>+</sup>CD4<sup>+</sup> cells (**a**) and CD45<sup>+</sup>CD4<sup>+</sup>CCR4<sup>+</sup>CCR8<sup>+</sup> Th2 cells (**b**) in hindlimb skin of mice from experiment depicted in Fig. 5c. **c, d** Representative FACS plots of single, live CD45<sup>+</sup>CD3<sup>+</sup>CD4<sup>+</sup> cells in ipsilateral inguinal lymph nodes (**c**) and hindlimb skin (**d**) of mice from experiment depicted in Fig. 5f. **e** Representative FACS plots of single, live CD4<sup>+</sup>CCR4<sup>+</sup>CCR8<sup>+</sup> Th2 cells in hindlimb skin of mice from experiment depicted in Fig. 5f.





**Supplementary Fig. 8. T cell cytokines promote the accumulation of iNOS-producing macrophages.** **a** Representative immunofluorescent images of tail cross-sections co-localizing LYVE-1<sup>+</sup> initial lymphatic vessels with CD11b<sup>+</sup> 6 weeks after tail skin and lymphatic excision; scale bar, 50 μm. **b** Quantification of CD11b<sup>+</sup> macrophages within 50 μm of LYVE-1<sup>+</sup> lymphatic vessels (n=4 for WT, n=5 for CD4KO and WT groups; 4 hpf/mouse). **c** Schematic diagram of macrophage isolation and subsequent *in vitro* treatment. **d** Representative FACS plots of single, live cultured CD45<sup>+</sup>CD11b<sup>+</sup>F4/80<sup>+</sup>CD11c<sup>-</sup>CD206<sup>-</sup> macrophages following isolation and prior to treatment. **e** PCR quantification of iNOS (*left*) and Arginase-1 (*right*) expression in cultured cells (n=2 for combined treatment, n=3 for no treatment, samples run in duplicate). **f** Representative immunofluorescent images co-localizing iNOS and F4/80 in cultured cells with insets representing magnified views; scale bars, 5 μm. Mean ± s.d.; \**P*<0.05, \*\**P*<0.01, and \*\*\**P*<0.001 by one-way ANOVA with Tukey's multiple comparisons test or student's *t* test. AT, CD4KO mice that underwent adoptive transfer with naïve CD4<sup>+</sup> T cells.